Eur. Phys. J. B **35**, 339–348 (2003)
DOI: 10.1140/epjb/e2003-00286-0

THE EUROPEAN PHYSICAL JOURNAL B

# NQR study of phase transitions in $CH_3HgX$ (X=Cl, Br, I)*

J. Pirnat[1,a], J. Lužnik[1], J. Seliger[2], Z. Trontelj[2], and D. Kirin[3]

[1] Institute of Mathematics, Physics and Mechanics, Univ. of Ljubljana, POB 2964, 1000 Ljubljana, Slovenia
[2] Fac. of Mathematics and Physics, Univ. of Ljubljana, POB 2964, 1000 Ljubljana, Slovenia
[3] R. Bošković Institute, POB 1016, 10001 Zagreb, Croatia

Received 16 January 2003 / Received in final form 23 June 2003
Published online 15 October 2003 – 

**Abstract.** The temperature dependence of halogen nuclear quadrupole resonance (NQR) in the series $CH_3HgX$ (X=Cl, Br, I) is measured with special emphasis on the structural phase transitions at $T_c$ = 162 K, 310 K, and ∼400 K, respectively. In the temperature dependences of NQR frequencies similarities are observed and discussed in relation with the structure and thermal vibrations on both sides of the phase transition. On the basis of known data a mechanism for the three analogous phase transitions is proposed. The chlorine spin-lattice relaxation behaviour in $CH_3HgCl$ can be explained by a competition of fast thermal fluctuations of MMX molecules across the high temperature (h.t.) mirror plane and of infrequent transitions to the other equivalent fluctuation mode across the orthogonal h.t. mirror plane. Proton high temperature relaxation is probably dominated by the same slow motion, but at lower temperatures some other mechanism involving magnetic coupling prevails.

**PACS.** 64.70.Kb Solid-solid transitions – 61.66.Fn Inorganic compounds – 76.60.Gv Quadrupole resonance

## 1 Introduction

Ecologists know $CH_3HgCl$ (methylmercury(II) chloride, MMCl) as a troublesome pollutant and as one of the initial steps in the metabolic chain of Hg poisoning. On the other hand, MMCl together with its halogen analogs $CH_3HgBr$ (MMBr) and $CH_3HgI$ (MMI) form an interesting series of rather similar, relatively simple compounds. Owing to the linear molecular shape (disregarding protons) these compounds have a simple scheme of molecular vibrations with a single torsional mode [1]. They are known to exhibit different structural phase transitions [1,2] in the solid state and are good paradigms for studying and modelling this type of phase transitions.

The aim of this research is to throw additional light, using halogen nuclear quadrupole resonance (NQR), upon Kirin's suggestion of an analogous sequence of isostructural phases at ambient pressure in methylmercury(II) chloride, bromide, and iodide [2]. This suggestion was made mainly on the basis of Raman measurements, available structural data, and space group analysis. The compatibility of our NQR frequency and relaxation data with the refined model of structural and dynamic changes on both sides of the orthorhombic-tetragonal phase transition is here questioned.

At ambient pressure one notices similarities in the Raman-spectra temperature dependences at the corresponding phase transitions: in MMCl at 162 K, in MMBr at 310 K, and in MMI at around ∼400 K [2]. The crystal structures of these compounds have been measured only at room temperature and ambient pressure. Figure 1 shows the tetragonal crystal structure of MMCl (space group *P4/nmm* [1–3]) and Figure 2 the orthorhombic structure of MMI (space group *Pmab*, in standard notation *Pbcm* [2]). Room temperature is well above the structural phase transition in MMCl and well below it in MMI. The assumption is that the structure in Figure 2 is isostructural with the low temperature structure of all three halides, while that in Figure 1 qualitatively corresponds to the high temperature phases. The phase transition is supposed to be driven by the softening of a phonon at the Brillouin-zone boundary. The $CH_3HgX$ molecules translationally move out of the mirror planes and the unit cell doubles. The structure *Pmab* may be represented by superposing the displacement modulation wave onto the high temperature structure. Its wavelength is commensurate with the structure. It equals twice the length of the high temperature unit cell. The crystal structure of MMBr, proposed in reference [1], slightly deviates from our scheme (rotational molecular displacements in

* Supported in part by the Ministry of Education, Science and Sport, Republic of Slovenia

[a] e-mail: janez.pirnat@imfm.uni-lj.si

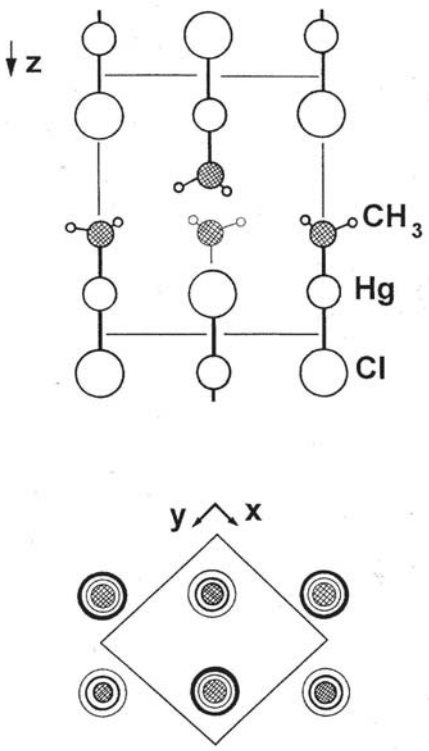


**Fig. 1.** Two orthogonal views (along (1,1,0) and along (0,0,1)) of the room temperature crystal structure of $CH_3HgCl$ ($P4/nmm$).

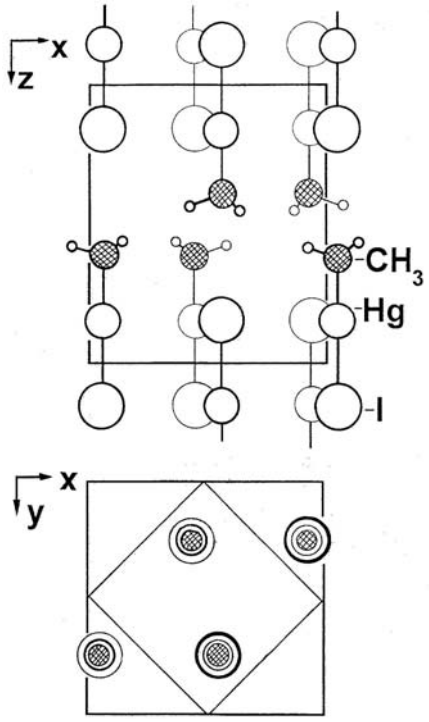


**Fig. 2.** Two orthogonal views (along (0,1,0) and along (0,0,1)) of the room temperature crystal structure of $CH_3HgI$ ($Pmab$).

the low temperature phase), but having been measured in the vicinity of the transition temperature of 310 K it might be less reliable for our purpose.

In the following we present our measurements of the temperature dependence of halogen NQR spectra. The observed similarities in MMCl, MMBr, and MMI NQR spectra are interpreted in relation with the proposed almost equal temperature activated sequences in the crystal structure. For MMCl, chlorine NQR relaxation and proton NMR relaxation measurements are also reported and discussed. A model of molecular fluctuations is proposed to explain the NQR temperature dependence and relaxation in both solid phases.

## 2 Measurements

According to our knowledge, only the halogen NQR frequencies at 77 K in the three MM halides (Cl, Br, and I) have been published [4,5]. Microwave determinations of the chlorine [6,7], bromine, and iodine quadrupole coupling constants (QCC) in the gas phase [8] are also known.

The temperature dependences of the halogen NQR spectra in commercial powder samples of MMCl, MMBr, and MMI (MMCl: Strem Chemicals, Newburyport, USA; MMBr: Alfa Aesar, Karlsruhe, Germany; MMI: two samples, Alfa Aesar and Strem Chemicals) were measured using a superregenerative NQR spectrometer [9] (Figs. 3a, b). Chlorine spectra were remeasured afterwards using the fast Fourier transform technique on a pulse NQR spectrometer (MATEC). At the same time, the temperature dependence of the chlorine NQR relaxation times $T_1$ and $T_2$ was obtained between 77 K and 300 K, as shown in Figure 4 (bromine and iodine NQR frequencies were outside the range of our pulse spectrometer).

In each compound we found two NQR lines: $^{35}$Cl and $^{37}$Cl lines in MMCl, $^{81}$Br and $^{79}$Br lines in MMBr, and two $^{127}$I lines ($1/2 \leftrightarrow 3/2$ and $3/2 \leftrightarrow 5/2$) in MMI. In Figure 3 only $^{35}$Cl, $^{81}$Br and the lower ($1/2 \leftrightarrow 3/2$) $^{127}$I resonances are shown. The isotope frequency ratios were as expected. The temperature dependences of Cl and Br NQR in the corresponding MM halides clearly confirm the expected phase transitions at 162 K and 310 K, respectively (Figs. 3a, b). In MMI with $^{127}$I as the only isotope we obtained the expected two single quantum NQR transitions. Our NQR data in this case reveal no solid-solid phase transition at ambient pressure below the melting temperature. The signal-to-noise ratio became too small above 360 K to continue with measurements of the iodine NQR temperature dependence. The spectral behaviour shows that the sample remains in the low temperature phase as long as the NQR signal is detectable.

We measured the $^{35}$Cl longitudinal relaxation by applying the standard method of recording free-induction-decay (FID) signal recovery after two $\pi/2$ pulses of variable separation and careful determination of the reference unsuppressed FID signal. The transverse relaxation $T_2$ was

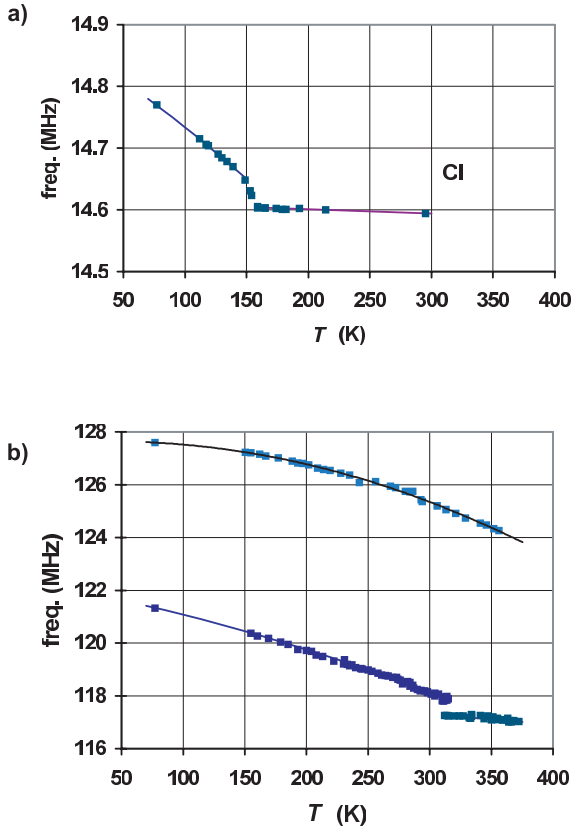


**Fig. 3.** a) Temperature dependence of the $^{35}$Cl NQR line in MMCl; b) temperature dependences of the $^{81}$Br and $^{127}$I NQR (1/2↔3/2) lines in MMBr and MMI. Trendlines are added as guides for the eyes. Note the departure from the smooth trendline in a) immediately below $T_c$.

obtained by measuring the quadrupole-echo signal after a $\pi/2 - \tau - \pi$ sequence of variable length.

For comparison, NMR spin-lattice relaxation in a magnetic field of 0.75 T was measured in MMCl [9,10]. All the relaxation results are collected in Figure 4.

## 3 Results and discussion

### 3.1 Quadrupole coupling constants

The quadrupole coupling constants of the halogen atoms in solid MMCl, MMBr, and MMI have relatively low values - 30 MHz, 240 MHz, and 850 MHz for $^{35}$Cl, $^{81}$Br, and $^{127}$I, respectively, as estimated assuming $\eta \sim 0$ (QCC $\simeq 2\nu_Q$ for $I = 3/2$ and QCC $\simeq \frac{20}{3}\nu_{Q(1/2\leftrightarrow 3/2)}$ for $I = 5/2$ [11]). On the basis of molecular and crystal likeness this is probably true although this small $\eta$ has really been determined only in the low temperature phase of the iodide ($I = 5/2$). The tendency to lowering the QCC from the "atomic" single $p$ electron values [12] increases from I to Cl, similarly to the electronegativity of the halogen atoms. One of the unquestionable reasons for the low quadrupole frequencies is therefore the ionic character of the Hg-X bond.

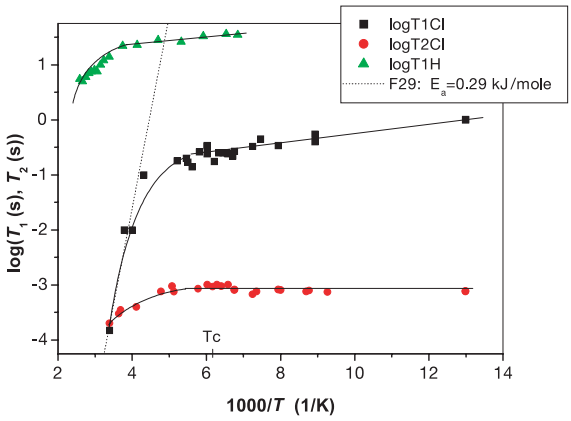


**Fig. 4.** Temperature dependence of $^{35}$Cl pure NQR longitudinal relaxation time $T_1$, the corresponding transversal relaxation time $T_2$, and proton spin-lattice relaxation time in an external magnetic field of 0.75 T.

The molecular QCCs in the gas state calculated from the microwave data [6,8] lie considerably higher than those obtained in the solid state. However, the strong ionicity $i$ of the bond has already been estimated in the gas state ($i$(Cl)∼62%, $i$(Br)∼55% [6]). In the solid phase there is an additional quadrupole-frequency lowering, called the crystal-field effect (usually about 5% [12]). It is the consequence of partial participation of the bonding electrons to intermolecular interactions in addition to intramolecular bonding. Again, the crystal-field effect is largest in MMCl (25%).

Measurement of the halogen QCC asymmetry parameter is not easy in MMCl and MMBr because of the nuclear spin of 3/2. However, for the tetragonal phase the structural symmetry at the halogen site (4-fold axis, mirror plane) requires an asymmetry parameter of 0. As mentioned above, the asymmetry parameters in the orthorhombic phases of MMCl and MMBr probably deviate from 0 but behave similarly to the one in MMI.

In MMI, the low temperature NQR spectral behaviour persists up to 360 K and no phase transitions were detected *via* the iodine NQR. Nevertheless, the NQR measurement in MMI is especially interesting because $^{127}$I has a spin $I = 5/2$. From the two quadrupole-resonance frequencies and their temperature dependences the temperature dependence of the asymmetry parameter $\eta$ in the *Pmab* phase was obtained. The asymmetry parameter provides information about the asymmetric environment of the I nucleus in that phase. The experimental data indicate a rather small, roughly unchanged asymmetry parameter between 0.023 and 0.033 in the temperature interval from 200 K to 360 K.

### 3.2 Structural aspects

Microwave investigations prove that the MMX molecular structure [6,8] in the gas phase is qualitatively similar to that in the solid state crystal structure. The gas molecules are linear with a covalent –Hg–$CH_3$ bond and a partly

| | | |
|---|---|---|
| | $CH_3$(0,a,-c) | |
| $CH_3$(-a,0,-c) | | $CH_3$(a,0,-c) |
| | $CH_3$(0,-a,-c) | |

| | | |
|---|---|---|
| X (-a,a,0) | Hg (0,a,0) | X (a,a,0) |
| Hg (-a,0,0) | X (0,0,0) | Hg (a,0,0) |
| X (-a,-a,0) | Hg (0,-a,0) | X (a,-a,0) |

| | | |
|---|---|---|
| Hg (-a,a,d) | X (0,a,d) | Hg (a,a,d) |
| X (-a,0,d) | Hg (0,0,d) | X (a,0,d) |
| Hg (-a,-a,d) | X (0,-a,d) | Hg (a,-a,d) |

**Fig. 5.** Crystal coordinates of some MMX atoms and groups, $Hg^+$, $X^-$ and $CH_3$ in the tetragonal phase in a suitable coordinate system of the orthorhombic crystal group *Pmab* (in MMCl $a$(Hg Cl) = 327 pm, $c$(Hg-C) = 206 pm, $d$(Hg-Cl) = 250 pm).

ionic –$Hg^+$–$X^-$ bond. In both solid phases at ambient pressure the MMX molecules are arranged in layers, as already mentioned. Each linear molecule, orthogonal to the layer, projects its methyl group into the interlayer space (Figs. 1, 2, 5). To minimize the electrostatic energy, the four nearest neighbours of each molecule have antiparallel directions of their –$Hg^+$–$X^-$ electric dipoles. An environment in which each $X^-$ ion is surrounded by 4 neighbouring $Hg^+$ ions, in addition to the one directly bound (above $T_c$ the site symmetry is $C_{4v}$), contributes to the increased ionic character of the –$Hg^+$–$X^-$ bond, especially in the case of Cl. Following Kirin's suggestion [2], in the high temperature phase the structures are tetragonal *P4/nmm* and each layer contains a square (quasi 2-dimensional) lattice of orthogonal linear molecules. The thermal motion of the $CH_3$ groups is rapid and their 3-fold symmetry incompatible with *P4/nmm* is time-averaged out. Neglecting the mutual interactions of the $CH_3$ groups, it is to be expected that within each layer the antiparallel $Hg^+$–$X^-$ electric dipoles form the lowest energy 2-dimensional lattice – the square lattice (unit length $a$). At lower temperatures, however, it is apparent that the orthorhombic *Pmab* structure with a rectangular 2-dimensional lattice in the layers becomes energetically more stable. The internal energy terms favouring an orthorhombic arrangement over a tetragonal one must be connected with the methyl groups.

The high-temperature-phase methyl interlayer consists of two displaced square lattices with double unit length and opposite orientation of the $CH_3$ groups. The $CH_3$ protons are very mobile with undefined positions near the C atoms along the $\cdots H_3\ H_3\ H_3 \cdots$ straight chains, running between the layers in $x$ and $y$ directions orthogonally to the molecular axes (see Figs. 1 and 6). For the sake of simplicity, we adopted the low temperature structure coordinate system (*Pmab*) in Figure 6.

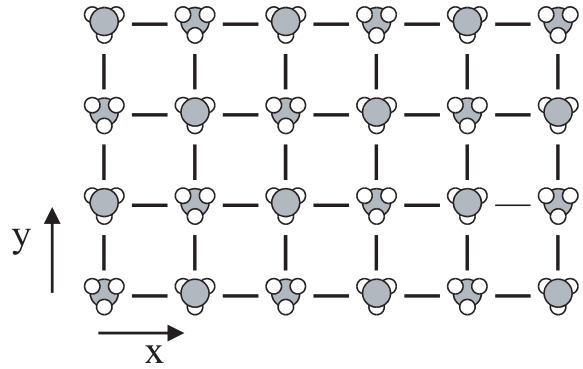


**Fig. 6.** Schematic high temperature averaged structure of the $CH_3$ interlayer with orthogonal $CH_3$ chains (the small circles do not indicate the protons' actual positions, which are undefined). For the sake of simplicity, the low temperature *Pmab* coordinate system is adopted.

Nonelectrostatic interactions between the methyl groups seem to prefer $\cdots H_3\ H_3\ H_3 \cdots$ chain folding which is also better compatible with the 3-fold symmetry. Below $T_c$ (162 K for Cl, 310 K for Br, 400 K for I), the whole $CH_3HgX$ molecule is laterally displaced out of the former 4-fold symmetric axis, which leads to a "diagonal" interchain nearing and which increases the number of $CH_3$ first shell neighbours from 4 (straight chains, Fig. 6) to 6 (folded chains, Fig. 7). It is indicative that relatively small molecular displacements in the $x$ direction, 25 pm for MMCl, are required for the distances ($CH_3 \leftrightarrow CH_3$) of the first and the second nearest neighbours to equalize (see Fig. 7). The tendency to displacement can be described by a semiempirical repulsion correction at the bottom of the potential well encaging the molecule, just at the crossing of the two orthogonal mirror planes (Fig. 8).

At lower temperatures such a shifted conformation seems to decrease the lattice internal energy beyond the simultaneous partial increase of electrostatic energy in the HgX layers. The low temperature structure can be achieved with molecular shifts in one of two equivalent orthogonal directions $x$ or $y$ (Fig. 7). The choice is a collective property of the domain thus formed.

In the following we refine Kirin's assumption of analogous phase transitions in the MMX family in the sense that the relevant crystal structures exist only as time averages of fluctuating low temperature local structures. The

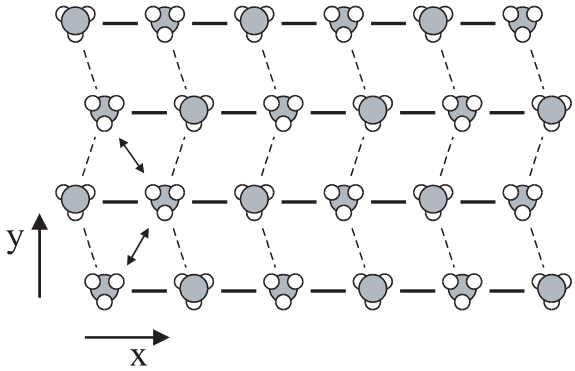


**Fig. 7.** Schematic low temperature interlayer averaged structure with displaced $CH_3$ groups and with changed "diagonal" interchain distances (two approaching $CH_3$ groups signed by ↔; the small circles do not indicate the protons' actual positions).

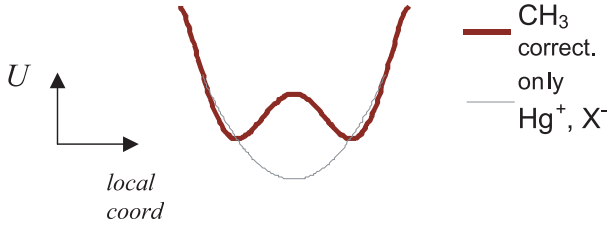


**Fig. 8.** One-dimensional projection of the monocentric potential well (only electrostatic forces and ionic short range repulsion, ——) and postulated $CH_3$ correction (▬).

incomplete crystallographic data [1–3] does not allow to decide between both possibilities, the formerly suggested displacive model of phase transitions and the present, order-disorder type. The mutual relations of the two models and the crossover between them has been frequently discussed over the past 10 years [13–21].

The instantaneous local structure presumably comprises slight displacement of MMX molecules from the 4-fold axis of the crystal group *P4/nmm* owing to the incompatible 3-fold symmetry of the $CH_3$ groups. The lateral molecular displacements are agitated along the covalent Hg–C bonds by the vivid intermolecular interactions in the $CH_3$ interlayers which usually remain mobile below 80 K. Our model therefore assumes layers of quadratic network of 4-fold originally symmetric quadruple potential wells, like the one shown in Figure 8. After placing the MMX electric dipoles loosely into the potential wells their mutual electrostatic interactions affect the combined potential around each molecule which thus can become asymmetric. In the high temperature phase the highly excited molecular fluctuations are symmetric so that the averaged MMX position is along the 4-fold axis. Below $T_c$, the molecular movement becomes asymmetric and in time average it results shifted MMX positions.

These assumptions overcome difficulties in explaining quadrupole measurements using the displacive model, in particular the explicit reduction of the temperature coefficient of the halogen NQR line above $T_c$. Below $T_c$, after shifting of the MMX molecule out of the mirror plane, the NQR frequency and the leading principal value of the EFG tensor increase considerably. In the displacive model to obtain zero temperature coefficient above $T_c$, thermal vibrations of the principal direction should just compensate the increase of the leading instantaneous principal value when the MMX molecule moves out of the mirror plane. It is not very probable that such a coincidence would occur both in MMCl as well as in MMBr.

The measurements of halogen $T_1$ also speak against the applicability of the displacive model for these compounds. When cooling the sample from the tetragonal phase across $T_c$, the critical slowing down of the displacement modulating phonon at $T_c$ should cause a dip in the halogen $T_1$ which is not noticed. Instead, the halogen longitudinal relaxation time slowly and uniformly increases across $T_c$.

In our model above $T_c$, owing to intermolecular couplings the lattice develops dynamic clusters, in which MMX molecules quickly fluctuate between the two opposite minima on both sides of the central position in one direction only. After the choice of the low temperature configuration with straight chains in the $x$ direction (as in Fig. 7) the two remaining minima along the orthogonal $y$ axis become less favourable, so the transition to the $y$ fluctuation occurs relatively rarely, and cooperatively with the neighbourhood. However, the probabilities of $x$ and $y$ fluctuations in the crystal are exactly the same. The most probable mechanism for a fluctuation direction change is movement of the cluster border. These symmetric fluctuations correspond to the high temperature phase, where the average positions of the molecules fall into the 4-fold axes as required by the symmetry group *P4/nmm* (the averaged structure is shown in Fig. 6).

According to our model, the X-ray diffraction should show a spatially averaged instantaneous picture of the tetragonal phase – slightly split 4-fold symmetrical MMX positions in the 4 potential minima around the $C_{4v}$ axis. The latter has not been reported so far but a small unexpected effect could have been overlooked.

When cooling the system across the solid-solid phase transition the model proposes that the fast symmetric molecular fluctuations between the two minima of the potential well do change. The intermolecular couplings start favouring one of the lower two potential minima, and this lowers its energy level, increases its occupation probability, and also prevents a change of fluctuation direction. In short, below the solid-solid transition the previously mobile fluctuation-direction domain boundaries freeze and at the same time the fluctuations become asymmetric. Figure 9 elucidates our model of the symmetric fluctuations and moving cluster border above $T_c$ (a) and the asymmetric fluctuations with frozen domain wall (b).

The critical temperatures in the MMX series at ambient pressure are shown in Table 1. The sequence of decreasing melting points from Cl to I is qualitatively consistent with the expected decreasing depth of the potential well and the decreasing electronegativity of the halogen atom in the same sense. The solid-solid transition

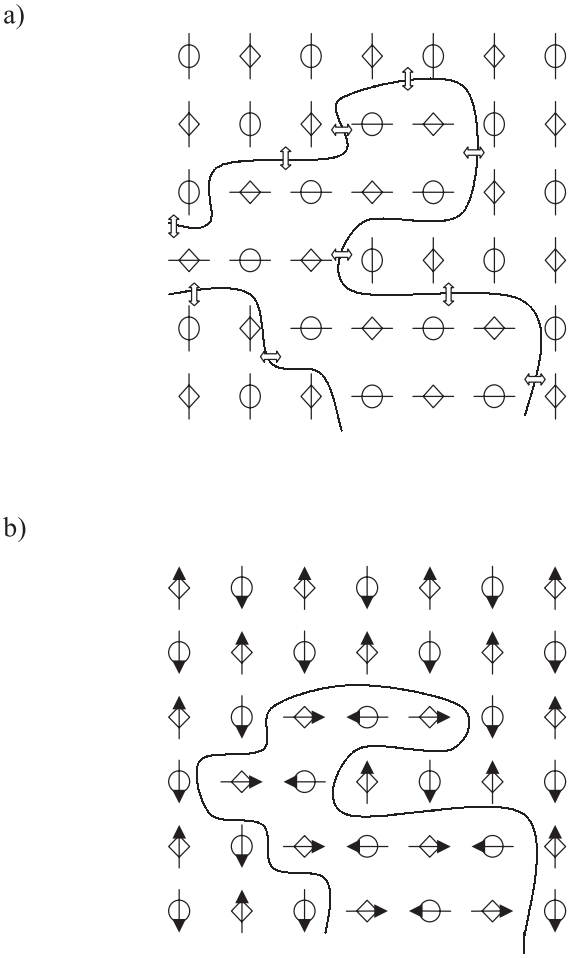


**Fig. 9.** Schematic illustration of the fluctuations in HgX layer (◇ HgX, ○ XHg): a) symmetric fluctuations and fluid cluster border between two areas with orthogonal directions of fluctuations above $T_c$; b) frozen domain wall and partly polarized sublattices with fast asymmetric fluctuations below $T_c$.

**Table 1.** Melting points and solid-solid phase transition temperatures $T_c$ in the MMX series.

| | Melting point [K] | $T_c$ [K] |
|---|---|---|
| MMCl | 443 | 162 |
| MMBr | 434 | 310 |
| MMI | 416 | ∼400 |

temperatures $T_c$, however, increase from Cl to I. These are the temperatures below which each molecular displacement begins to adapt to the neighbouring displacements. This influence therefore increases from Cl to I.

A recently published article on extended Raman investigations in MM halides [22] reports additional changes in the Raman spectra attributed to $CH_3$ interactions, which deserve further attention.

### 3.3 NQR and the structural phase transition

Using the above model we shall derive the Cl NQR temperature dependence in MMCl. Let the MMCl molecule fluctuate between the two sites located symmetrically at $u_x$ and $-u_x$ on both sides of the high temperature mirror plane. The fluctuation is fast on the NQR frequency scale also below $T_c$. It is asymmetric so that one side is favoured. We assume temperature independence of the fluctuation amplitude. This is acceptable in the first approximation because it only means a constant distance between the opposite minima of the potential well. However, the occupation probability and fluctuation rate change with temperature. Above $T_c$ the occupation probabilities of the two opposite minima equalize. The fluctuation rate increases. Besides, another motion gradually enters, namely infrequent transitions to the orthogonal fluctuation mode between the displacements $u_y$ and $-u_y$. After the transition, the fast fluctuations in the $y$ direction are equivalent to those in the $x$ direction. The relaxation measurements show that these transitions probably occur rarely compared to the NQR frequency (Sect. 3.4). An analogous model could be applied to MMBr and MMI; however, there the relaxation data are lacking for support and comparison.

We assume that the molecular shift $\pm u_x$ from the mirror plane is accompanied by an inclination from that plane by a small angle $\pm\theta$, and similarly in the case of the orthogonal shift $\pm u_y$. Also assuming the molecular asymmetry parameter $\eta = 0$ and a locking of the tensor principal axis to the molecular long axis, we obtain the modified electric field gradient (EFG) tensor at $\pm u_x$:

$$\mathbf{V}_{\pm u_x} \simeq \begin{pmatrix} V_{ZZ0}(\frac{3}{2}\theta^2 - \frac{1}{2}) & 0 & \pm\frac{3}{2}V_{ZZ0}\theta \\ 0 & -\frac{1}{2}V_{ZZ0} & 0 \\ \pm\frac{3}{2}V_{ZZ0}\theta & 0 & V_{ZZ0}(1 - \frac{3}{2}\theta^2) \end{pmatrix}. \tag{1}$$

Here, $V_{ZZ0}$ means the largest principal value of the static EFG tensor.

Above $T_c$, owing to fast symmetric fluctuations between the two values, the effective averaged EFG tensor becomes diagonal:

$$\langle \mathbf{V}_{\pm u_x} \rangle \simeq \begin{pmatrix} V_{ZZ0}(\frac{3}{2}\theta^2 - \frac{1}{2}) & 0 & 0 \\ 0 & -\frac{1}{2}V_{ZZ0} & 0 \\ 0 & 0 & V_{ZZ0}(1 - \frac{3}{2}\theta^2) \end{pmatrix}. \tag{2}$$

The orthogonal fluctuating mode ($\pm u_y$) results in almost the same averaged EFG tensor with permuted elements $V_{xx}$ and $V_{yy}$. If the transitions between the two modes are rare compared to the NQR frequency, the NQR spectrum will be a superposition of the contributions of both averaged tensors. However, the differences between the two cannot be resolved without the Zeeman perturbed NQR in a single crystal. Axial asymmetry of the EFG tensor in the high temperature phase could be easily experimentally proved only in MMI, but there the iodine NQR signal already disappeared in the low temperature phase.

If $\theta$ is temperature independent the quadrupole frequency above $T_c$ is constant, which is in accordance with the unusually low experimental temperature coefficients for Cl and Br (relative values $\sim 5 \times 10^{-6}$/K and $\sim 3 \times 10^{-5}$/K, respectively; the relative slope changes at

$T_c$ are 24 : 1 and 4.5 : 1 ):

$$\nu_Q(T \geq T_c) = \nu_Q(T_c) = \nu_0 \left(1 - \frac{3}{2}\theta^2\right). \quad (3)$$

Here, $\nu_0$ is the NQR frequency of a static molecule and for an estimate of its magnitude we can assume that the asymmetry parameter $\eta$ is negligibly small, which will be justified in the following.

Below $T_c$ we assume that the transitions between the two orthogonal modes die out. Our quadrupole probe still senses the average EFG between the two remaining opposite sites across the mirror plane, except that the average is now weighted with the occupation probabilities $\frac{1+S}{2}$ and $\frac{1-S}{2}$:

$$\langle \mathbf{V}(T < T_c) \rangle = \frac{(1+S)}{2}\mathbf{V}_{u_x} + \frac{(1-S)}{2}\mathbf{V}_{-u_x}. \quad (4)$$

where $S$ is the so-called order parameter, equal to 0 at $T_c$ and growing towards 1 with decreasing temperature.

Combining equation (1) and equation (4) we obtain

$$\langle \mathbf{V}(T < T_c) \rangle = \begin{pmatrix} V_{ZZ0}(\frac{3}{2}\theta^2 - \frac{1}{2}) & 0 & \frac{3}{2}V_{ZZ0}\theta S \\ 0 & -\frac{1}{2}V_{ZZ0} & 0 \\ \frac{3}{2}V_{ZZ0}\theta S & 0 & V_{ZZ0}(1 - \frac{3}{2}\theta^2) \end{pmatrix}. \quad (5)$$

Diagonalizing this tensor the largest principal value can be approximated as

$$V_{ZZ} \simeq V_{ZZ0}\left(1 - \frac{3}{2}\theta^2 + \frac{3}{2}\theta^2 S^2\right). \quad (6)$$

This is valid in both solid phases, with $S = 0$ above $T_c$. The NQR frequency can be expressed as

$$\nu_Q \simeq \nu_Q(T_c) + \frac{3}{2}\nu_0\theta^2 S^2\,, \quad (7)$$

where $\nu_0$ is the NQR frequency of a "static" molecule. For an estimate of $\theta^2$ from equation (7) we extrapolate $\nu_0 \simeq \nu(0\ \mathrm{K}) = 14820\,\mathrm{kHz}$ and take $\nu_Q(T_c) = 14602\,\mathrm{kHz}$, resulting in

$$\theta^2 \simeq \frac{2}{3} \cdot \frac{\nu_0 - \nu_Q(T_c)}{\nu_0} = \frac{145}{14820}\ ;\ \ \theta \simeq 6^0. \quad (8)$$

We stress that this tilt angle actually corresponds to the fluctuation of the principal direction of the EFG tensor. The working hypothesis was that the EFG principal axis is locked to the molecular axis. However, those two directions can easily deviate by some degrees owing to the influences of neighbouring polar molecules and even more owing to electronic redistributions [12]. The molecular fluctuation could take only a part of the calculated EFG tilt angle $\theta$. Consequently, by smaller molecular displacement and longer fluctuation cycle ($(\tau_{+-} + \tau_{-+})$, see Sect. 3.4) the required energy for molecular oscillator excitation is lower than expected at first. In the following section it will be clear that with the order parameter $S = 0.9$

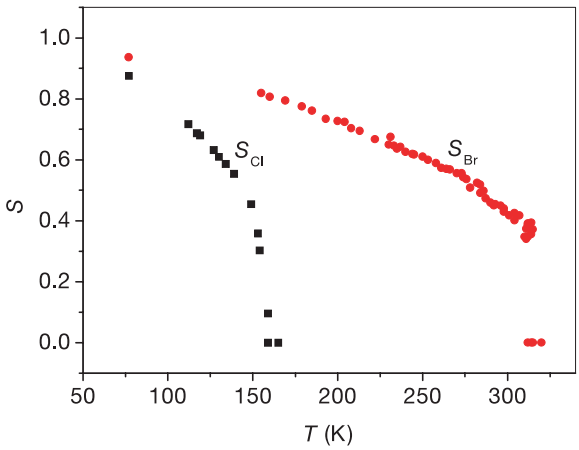


**Fig. 10.** Temperature dependence of the order parameter in MMCl and in MMBr.

(it corresponds to $T \sim 80$ K) we obtain the fast fluctuation cycle time of about $10\tau_f$ ($\tau_f$ is the correlation time determined in Section 3.4 from Cl $T_1$, approximately equal to the less probable molecular occupation time). Assuming that the quickly rotating and interacting $CH_3$ groups, covalently bound to HgX groups, enhance fluctuations of the latter, it is obvious that our model can be applied to MMCl, MMBr, and MMI.

With the above model, the EFG tensor asymmetry parameter $\eta$ takes the largest value at $T \geq T_c$. Below $T_c$ it gradually decreases with increasing $S$. However, above $T_c$ the symmetry group *P4/nmm* requires the time-averaged asymmetry of the EFG tensor equal to 0. But above $T_c$ the transitions between the orthogonal fluctuation modes are so slow at the NQR time scale, that NQR measures the superposition of the NQR spectra of the two corresponding asymmetric tensors. In times much longer than $(\nu_Q)^{-1}$ those two average to an axially symmetric tensor. Below $T_c$, where the domains of the fluctuation direction become static, the capability of the NQR detection of the EFG asymmetry parameter in principle remains the same.

The experimental estimate of $\eta$ was possible only in the low temperature phase of MMI, where $\eta = 0.028 \pm 0.005$. This can be compared to the maximum asymmetry parameter in MMCl estimated from equations (2) and (8): $\eta \sim \frac{3}{2}\theta^2 \sim 0.01$.

Below $T_c$ the temperature dependence of the order parameter can be expressed from equations (7) and (3) as:

$$S(T < T_c) = \sqrt{\frac{\nu_Q(T) - \nu_Q(T_c)}{\nu_0 - \nu_Q(T_c)}}. \quad (9)$$

The diagrams of $S$ calculated from the experimental data for MMCl and MMBr are shown in Figure 10.

In MMCl the variations of the slope $\nu_Q$ *vs.* $T$ and of the order parameter immediately below $T_c$ are rather strong but an abrupt step is not obvious, though not excluded because of insufficient temperature stabilization ($\pm$1K). In MMBr the frequency and order parameter steps at $T_c$ are quite pronounced with relative sizes 0.06 and 0.04,

respectively. If the transition is of the $1^{st}$ order as indicated by the Raman data [1], one would expect an abrupt step at $T_c$.

### 3.4 Relaxation in MMCl

The temperature dependence of the $^{35}$Cl longitudinal relaxation time $T_1$ steadily decreases with increasing temperature with no abrupt irregularities at $T_c = 162$ K within experimental error, whereas in $T_2$ some variations are noticeable in this temperature region which may be ascribed to noise only (Fig. 4). For comparison, the results of measurements of proton NMR relaxation in an external magnetic field of 0.75 T in the temperature region around $T_c$ (150 K to 380 K) are also given in Figure 4 [10].

Looking at quadrupole longitudinal, transverse, and NMR spin-lattice relaxations of chlorine and protons, respectively, in the usual $\log T_{1,2}$ *vs.* $1/T$ plot (Fig. 4), we notice at first a rough similarity – in all cases the slope of the variation of $T_{1,2}$ increases with increasing temperature above $T_c$. The slope increase seems to be continuous in all cases. It occurs in the ∼50 K interval just above $T_c$ in the case of Cl $T_2$, maybe a few K higher in the case of Cl $T_1$, and the highest (about 90 K higher, namely near ∼250 K) in the case of the proton $T_1$.

Let us consider first the Cl spin lattice relaxation in MMCl in the light of the model so far discussed. In the quadrupole system, where the nondiagonal elements $\pm\frac{3}{2}V_{ZZ}\theta$ of the EFG tensor quickly fluctuate between the two values with probabilities $\frac{(1+S)}{2}$ and $\frac{(1-S)}{2}$ with an inverse correlation time $\tau_f^{-1} = (\tau_{+-})^{-1} + (\tau_{-+})^{-1}$, the following expression for the relaxation rate can be derived [23]:

$$\frac{1}{T_1} = 12(1+S)(1-S)\Big(\frac{\pi eQ}{h}\Big)^2 \cdot \frac{9}{4}V_{ZZ}^2\theta^2\frac{\tau_f}{1+(\omega_Q\tau_f)^2}\,. \tag{10}$$

where $\omega_Q = 2\pi\nu_Q$. Equation (10) can be rewritten taking Equation (7) into account:

$$\frac{1}{T_1} = 12\pi^2(1-S^2)\nu_0(\nu_0\theta^2)\frac{\tau_f}{1+(\omega_Q\tau_f)^2}\,. \tag{11}$$

From this we obtain an estimate for the temperature dependence of the correlation time $\tau_f$. This corresponds to the rapid fluctuations between the two symmetric molecular displacements from the mirror plane which dominate the Cl relaxation below $T_c$, and also slightly above it, where the order parameter becomes 0 but the transitions to orthogonal fluctuations ($\pm u_x \leftrightarrow \pm u_y$) are still negligible:

$$\frac{\tau_f}{1+(\omega_Q\tau_f)^2} \simeq \tau_f \simeq [12\pi^2(1-S^2)(\nu_0\theta)^2T_1]^{-1}\,. \tag{12}$$

Some ten K above $T_c$ the temperature dependence of the chlorine $T_1$ gradually increases its slope (Fig. 4). In our model, above $T_c$ the previously frozen boundaries between the domains with orthogonal fluctuation modes become more and more mobile and the slow transitions between the orthogonal fluctuation modes provide a new efficient relaxation mechanism. There are two contributions to the Cl spin-lattice relaxation rate now: the one from the fast fluctuations in a constant direction and a new one from the rarely changing direction of equally fast fluctuations:

$$\frac{1}{T_1} = \Big(\frac{1}{T_1}\Big)_{fast} + \Big(\frac{1}{T_1}\Big)_{slow}\,. \tag{13}$$

We presume that it is the slow process which causes the slope change in the $T_1$ temperature dependence. Some ten K above it becomes the dominant contribution to Cl spin-lattice relaxation. In the temperature interval from $T_c$ to the slope change, the two comparable contributions cannot be separated and the two correlation times $\tau_f$ and $\tau_s$ cannot be derived from $T_1$ independently.

Above $T_c$ the quadrupole probe senses the averaged EFG tensor (Eq. (5), $S = 0$)

$$\langle \mathbf{V}_{\pm u_x}\rangle \simeq \begin{pmatrix} V_{ZZ0}(\frac{3}{2}\theta^2 - \frac{1}{2}) & 0 & 0 \\ 0 & -\frac{1}{2}V_{ZZ0} & 0 \\ 0 & 0 & V_{ZZ0}(1-\frac{3}{2}\theta^2) \end{pmatrix}, \tag{14}$$

which temporarily changes to a tensor with equal diagonal values except that the elements $V_{xx}$ and $V_{yy}$ are permuted. The relaxation rate caused by such slow transitions can be written [24]:

$$\begin{aligned}\Big(\frac{1}{T_1}\Big)_{slow} &= \frac{1}{3}\Big(\frac{\pi eQ}{h}\Big)^2(\delta V_{xx} - \delta V_{yy})^2\frac{\tau_s}{1+(\omega_Q\tau_s)^2} \\ &= 3\pi^2\nu_0^2\theta^4\frac{\tau_s}{1+(\omega_Q\tau_s)^2}\,.\end{aligned} \tag{15}$$

Here $\tau_s$ means the correlation time for the high temperature relaxation mechanism – fluctuation-direction transitions. This correlation time can be estimated assuming that $\omega_Q\tau_s \gg 1$:

$$\begin{aligned}\frac{\tau_s}{1+(\omega_Q\tau_s)^2} \simeq \frac{1}{(\omega_Q^2\tau_s)} &= \Big[\frac{3}{2}\omega_Q^2\theta^4(T_1)_{slow}\Big]^{-1}; \\ \tau_s &\simeq \frac{3}{2}(T_1)_{slow}\theta^4.\end{aligned} \tag{16}$$

Figure 11 shows the temperature dependences of the two correlation times obtained from the experimental data using the proposed model. The correlation time for the fast fluctuations of molecules across the potential mirror plane seems to be almost temperature independent below $T_c$. This is acceptable if we note that in the case of different contributions $\tau_{+-}$ and $\tau_{-+}$, $\tau_f$ is approximately equal to the shorter life-time.

The long correlation time for the slow fluctuation-direction transitions, dominating the high temperature $T_1$, is obviously thermally activated (activation energy $E_a \sim 0.29$ kJ/mole). The room temperature $T_1$ measurement seems to indicate the vicinity of a $T_1$ minimum, but further measurements to confirm that assumption are missing because the NQR signal disappears in noise.

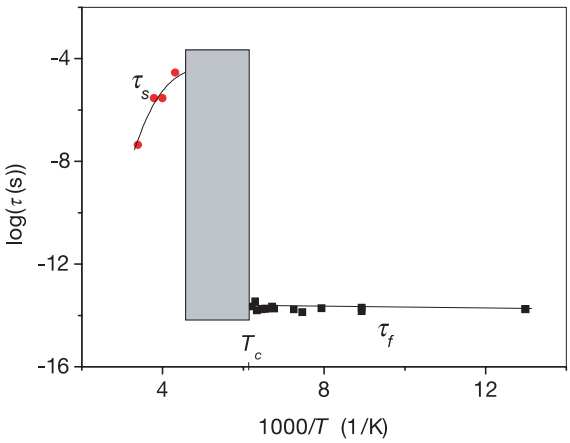


**Fig. 11.** Temperature dependence of the short and long correlation times, corresponding to the low temperature fast molecular fluctuations and high temperature slow transitions of fluctuation directions. In the shaded region both contributions to $T_1$ are comparable and the two correlation times cannot be determined.

To test whether the proton $T_1$ in a magnetic field of 0.75 T is dominated by the same mechanism as the Cl $T_1$, we can compare the measured $T_1$ ratio with the one estimated using the golden rule of time dependent perturbation theory [25]. Around room temperature the dominating motion with fluctuating terms $\Delta\omega_{\mathrm{H}}$ and $\Delta\omega_{\mathrm{Cl}}$ is relatively slow and $\frac{T_1(\mathrm{Cl})}{T_1(\mathrm{H})} \sim [\frac{\Delta\omega_{\mathrm{H}}}{\omega_{\mathrm{H}}} \frac{\omega_{\mathrm{Cl}}}{\Delta\omega_{\mathrm{Cl}}}]^2 \sim 10^{-5}$ to $10^{-6}$ which is fulfilled. Also the corresponding temperature coefficients approach each other at high temperatures. Therefore, above ∼280 K we expect the same dominant relaxation mechanism for the two nuclei, *i.e.* slow transitions between the fluctuation directions.

If the fast relaxing mechanism is to be the same for the two relaxations, below $T_c$ the ratio of the Cl and proton $T_1$ should be the same as the squared ratio of the absolute fluctuating terms $[\frac{\Delta\omega_{\mathrm{H}}}{\Delta\omega_{\mathrm{Cl}}}]^2 \sim 10^{-5}$ which is not the case. The proton $T_1$ is about 3 orders of magnitude shorter than expected, which means that protons sense some additional more efficient relaxing mechanism. A probable candidate for this which should simultaneously have only a small influence on Cl relaxation is presumably connected with the fast rotations of the $CH_3$ groups in the interlayer.

## 4 Summary

– The three methylmercury halides MMX (X=Cl,Br,I) have analogous molecular structures. The corresponding crystal structures are layered, with similar molecular arrangements, with stronger, long range electrostatic $Hg^+$ $Cl^-$ interactions and with weaker forces and fast thermal motion expected in the nonpolar $CH_3$ interlayers. Temperature dependences of halogen NQR frequencies below $T_c$ in MMCl, MMBr and MMI are qualitatively similar, which also holds true for MMCl and MMBr above $T_c$. The NQR signal for MMI disappears before the phase transition.

– The above features, together with the Raman measurements, support the assumption of similarities in the lattice dynamics of methylmercury halides, which play the principal role in averaging their halogen EFG tensors.

– The proposed model of the changing nature of competitive fast and slow fluctuations of the MMX molecules across the two orthogonal high temperature mirror planes is a refinement of Kirin's suggestion of the structural behaviour of MMX analogues. It qualitatively explains the small NQR temperature coefficient above $T_c$ and determines the connection between the temperature dependence of NQR below $T_c$ and the order parameter causing a preferred occupation on one side of the previous mirror plane. A possible stimulus agitating the relatively heavy HgX groups are the covalently bound, easily activated and mutually interacting $CH_3$ groups in the interlayers.

– The small asymmetry parameter measured in the orthorhombic crystal structure of MMI is qualitatively consistent with the calculated low temperature value of MMCl, resulting from our model.

– The model also explains the gentle slope in Cl spin-lattice relaxation below $T_c$ and slightly above it by fast fluctuations across the potential mirror plane, and the steep region above $T_c$ by slow transitions between the orthogonal fluctuation directions. The latter, a strongly thermally activated relaxation mechanism, is probably also effective in proton high temperature relaxation, whereas the low temperature proton relaxation should probably be ascribed to some motion connected with $CH_3$ rotation.

We are much obliged to Mr. V. Žagar, Jožef Stefan Institute, Ljubljana, for the measurements of the proton NMR relaxation.

## References

1. D.M. Adams, M. Pogson, J. Phys. C: Solid State Phys. **2**, 1065 (1988)
2. D. Kirin, Phys. Rev. B **58**, 2353 (1998)
3. D.R. Grdenić, A.I. Kitaigorodsky, Zh. Fiz. Khim. **23**, 1161 (1949)
4. G.K. Semin, T.A. Babushkina, G.G. Yakobson, *Primenenie jadernogo kvadrupolnogo rezonansa v himii* (Himia, Leningrad, 1972)
5. E.V. Bryuhkova, A.K. Prokof'ev, T.Y. Mel'nikova, O.Y. Okhobystin, G.K. Semin, Izv. Akad. Nauk SSSR, Ser. Khim. p. 477 (1974)
6. W. Gordy, J. Sheridian, J. Chem. Phys. **22**, 92 (1954)
7. C. Feige, H. Hartmann, Z. Naturforschung a **22**, 1286 (1967)
8. C. Walls, D.G. Lister, J. Sheridian, J. Chem. Soc., Faraday Trans. II **71**, 1091 (1978)
9. J. Pirnat, J. Lužnik, Z. Trontelj, D. Kirin, in *Proceedings of Ampere Summer School "Applications of Magnetic Resonance in Novel Materials"*, edited by G. Papavassiliou (2000), p. 130
10. J. Pirnat, Z. Trontelj, J. Lužnik, D. Kirin, Z. Naturforsch. a **55**, 215 (2000)

11. T.P. Das, E.L. Hahn, in *Nuclear Quadrupole Resonance Spectroscopy, Solid State Physics, Suppl. 1*, edited by F. Seitz, D. Turnbull (Academic Press, New York, London, 1958), p. 14
12. E.A.C. Lucken, *Nuclear Quadrupole Coupling Constants* (Academic, London, 1969)
13. R. Blinc, B. Žekš, in *Selected Topics in Solid State Physics,* Vol. XIII, edited by E.P. Wohlfarth (North Holland, Amsterdam, 1974)
14. A. Bussmann-Holder, J. Phys. Chem. Solids **57**, 1445 (1996)
15. A. Bussmann-Holder, N. Dalal, K.H. Michel, J. Phys. Chem. Solids **61**, 271 (2000)
16. M. Jochum, H.-G. Unruh, Eur. Phys. J. B **5**, 163 (1998)
17. M. Ichikawa, T. Gustafsson, I. Olovsson, Solid State Commun. **123**, 135 (2002)
18. G. Völkel, N. Alsabbagh, R. Böttcher, D. Michel, B. Milsch, Z. Czapla, J. Furtak, J. Phys.: Condens. Matter **12**, 4553 (2000)
19. D. Merunka, B. Rakvin, Phys. Rev. B **66**, 174101 (2002)
20. A. Proykova, R. S. Berry, Eur. Phys. J. D **9**, 445 (1999)
21. A.N. Rubtsov, J. Hlinka, T. Janssen, Phys. Rev. B **61**, 126 (2000)
22. V. Mohaček-Grošev, D. Kirin, Eur. Phys. J. B **20**, 85 (2001)
23. J. Seliger, R. Blinc, J. Phys.: Condens. Matter **5**, 9401 (1993)
24. J. Seliger, Sol. State NMR **8**, 207 (1997)
25. E. Merzbacher, *Quantum Mechanics* (Wiley & Sons, Inc., New York, 1961)